J Clust Sci (2007) 18:720–728
DOI 10.1007/s10876-007-0145-6

ORIGINAL PAPER

On the Electronic Structure of Distorted Cubic Rhodium Cluster Complexes Containing Bridging Germanium or Phosphorus Ligands

Bachir Zouchoune · Jean-Yves Saillard · Jean-François Halet

Received: 2 April 2007 / Published online: 27 July 2007

Abstract DFT calculations show that the optimal metal valence electron (MVE) count of omnicapped cubic rhodium clusters containing more than eight terminal ligands, is 114. For such a count, a closed-shell configuration is computed with a substantial HOMO-LUMO gap. The presence of more than eight terminal ligands in the clusters favors highly distorted cubic architectures with capping ligands asymmetrically bound to the distorted metallic square faces. Removal of terminal ligands leads to the replacement of bonding M–L electron pairs by nonbonding electron pairs localized on the metal atoms, giving rise to unchanged MVE count.

Keywords Electronic structure · DFT calculations · Transition metal clusters

Introduction

Although the octahedral M_6 structural arrangement is by far the most abundant in ligand-stabilized transition-metal cluster chemistry, a fascinating class of cubic compounds has emerged over the last years [1]. It turns out that the usual electron-counting rules, such as those based on the effective atomic number (EAN) approach or the polyhedral skeletal electron pair (PSEP) theory [2], are in general limited for rationalizing the structure and bonding of this kind of cluster [1]. This is simply

B. Zouchoune
Laboratoire de Chimie Appliquée et Technologie des Matériaux, Centre Universitaire Larbi Ben M'Hidi, 04000, Oum-El-Bouaghi, and Laboratoire de Chimie Moléculaire, du Contrôle de l'Environnement et des Mesures Physico-Chimiques, Université-Mentouri de Constantine, Constantine, 25000, Algeria

B. Zouchoune (✉) · J.-Y. Saillard · J.-F. Halet (✉)
Sciences Chimiques de Rennes, UMR CNRS 6511, Université de Rennes 1, Rennes Cedex, 35042, France
e-mails: bzouchoune@yahoo.com; halet@univ-rennes1.fr

because electron-counting rules are based on the principle of closed-shell requirement, which associates to a given molecular structure one favored electron count corresponding to a significant HOMO-LUMO gap, and conversely. It turns out that in highly compact clusters, structural changes arising from varying the electron count are damped by the high connectivity of the molecular cage. As a consequence, to a given cluster structure may sometimes correspond a range of allowed electron counts, not all of them obeying the closed-shell principle. Such a situation is reminiscent of what is often observed in solid-state chemistry. The upper limit of this range is often well defined and corresponds to the best-favored closed-shell electron count for the considered structure. This is what is observed in cubic clusters of the type $M_8L_8(\mu_4\text{-}E)_6$ or $M_8L_8(\mu_4\text{-}ER)_6$ (M = transition metal, L = two-electron donor ligand, and E = group 14, 15, and 16 element) for which the upper allowed limit number of metal valence electrons (MVE) is 120. This closed-shell electron count is predicted by the EAN and PSEP rules. Experimentally, the same structural arrangement is found for MVE counts varying from 120 down to 99. Some expansion or shrinking of the cube is simply observed upon variation of the number of MVEs. Similarly, MVE counts between 121 and 130 have been observed so far in the case of metal-centered $M_9L_8(\mu_4\text{-}E)_6$ or $M_9L_8(\mu_4\text{-}ER)_6$ species [3–5]. Distorted cubic arrangements are also encountered when the ligand environment of the metallic cage is nonsymmetrical. This is observed for instance in the 127-MVE cluster $[Co_9(CO)_{16}(\mu_5\text{-}Bi)_4]^{2-}$ and the 130-MVE compound $Pd_9(PPh_3)_8(\mu_4\text{-}As_2)_4$ where only four of the six faces are capped [6, 7].

Distortion is also encountered for omnicapped species having more than eight terminal ligands such as in the octanuclear germanilidene or phosphinidene rhodium clusters $Rh_8(CO)_{12}(\mu_4\text{-}GePh)_6$ (**1**), $Rh_8(CO)_8(PPhMe_2)_4(\mu_4\text{-}GePh)_6$ (**2**) recently characterized [8], and $Rh_8(CO)_9(\mu_4\text{-}P(C_5H_9))_6$, (**3**) [9]. These compounds are shown in Scheme 1 where the Ph and C_5H_9 groups are omitted for clarity. Surprisingly, all these three species possess 114 MVEs ($9(Rh) \times 8 + 2(CO) \times 12 + 3(GePh) \times 6$ for **1**, $9(Rh) \times 8 + 2(CO) \times 8 + 2(PPhMe_2) \times 4 + 3(GePh) \times 6$ for **2**, and $9(Rh) \times 8 + 2(CO) \times 9 + 4(P(C_4H_9)) \times 6$ for **3**), which, as said earlier, are six electrons less than the expected count of 120. Interestingly, the count of 114 MVEs is also adopted by uncapped octanuclear clusters containing π-acceptor ligands such as the carbon-centered $[Co_8(CO)_{18}(\mu_8\text{-}C)]^{2-}$, which depicts a distorted square

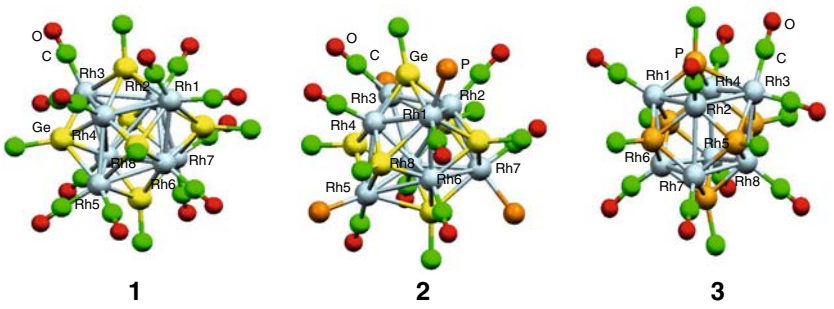

Scheme 1 Experimentally characterized 114-MVE cubic clusters

antiprimatic polyhedron [10], or $Rh_8(CO)_{19}(\mu_8\text{-C})$ which adopts a capped trigonal prismatic array [11].

The fact that **1**, **2** and **3** have the same electron count but a different number of extra two-electron ligands tethered to the metal atoms, either one or two, is puzzling. This prompted us to undertake their theoretical analysis with the aid of density functional theory (DFT) calculations in order to understand the origin of the Rh_8 core distortion and to define the role of the number of two-electron ligands in the stability of these species. The main results are discussed in this paper.

Computational Details

DFT calculations were carried out using the Amsterdam Density Functional (ADF) [12] package developed by Baerends and coworkers [13]. The results discussed in this paper were obtained assuming the local density approximation of electron correlation using the Vosko–Wilk–Nusair parameterization [14] and nonlocal density approximation with Becke [15] and Perdew [16] corrections for the exchange and correlation energies, respectively. Geometry optimizations were based on the method developed by Versluis and Ziegler [17]. The standard ADF basis set TZP was used for the atoms, which describes the valence 4d (Rh), 5s (Rh), 5p (Rh), 3d (Ge), 4s (Ge), 4p (Ge), 3s (P), 3p (P), 2s (C), 2p (C), and 1s (H) orbitals with triple-ζ Slater-type orbitals. The frozen-core approximation was used to treat the core electrons. The integration accuracy parameter was set to six. The convergence criteria were the following: 0.001 Hartrees for the changes in the energy, 0.01 in Hartree/Å for the changes in gradients, and 0.01 Å for the changes in the Cartesian coordinates. The Coulomb potential was evaluated *via* an accurate fitting of the charge density with Slater-type exponential functions centered on the atoms [13]. To reduce computational effort, calculations were carried out on different models by replacing GePh, $P(C_5H_9)$, and $PPhMe_2$ ligands by GeH, PH, and PH_3, respectively.

Results and Discussion

The structural arrangement of compounds **1** and **2** consists of a distorted cube of eight rhodium atoms and six phenylgermanium groups that quadruply bridge each face (Scheme 1) [8]. There are no bridging carbonyls in these compounds. The 12 "cube" edges correspond to Rh–Rh bonding distances ranging from 2.8208(7) to 2.9397(8) Å in the former and from 2.8660(18) to 2.9585(18) in the latter. The"cube" is made of two interpenetrating tetrahedral made of four $Rh(CO)_2$ [or four $Rh(CO)(PPhMe_2)$] and four Rh(CO) fragments, respectively. The tetrahedrally distorted cube exhibits weak Rh–Rh interactions along four diagonals that range from 3.158(1) to 3.264(1) Å in **1** and from 3.277(2) to 3.395(2) Å in **2**. This distortion is most likely caused by the fact that four of the rhodium atoms have two terminal ligands while the other four have only one carbonyl ligand. Each germanium atom asymmetrically binds to four rhodium atoms with distances

spanning a wide range, i.e., two short bonds, ca. 2.3–2.4 Å and two long bonds, ca. 2.5–2.8 Å [8].

The molecular geometry of compound **3** consists of a slightly distorted rhodium cube capped on each face by a phosphinidene group (Scheme 1). Each Rh atom bears one terminal CO ligand except one, which has two [9]. The Rh–Rh distances all range from 2.712(3) to 2.881(3) Å**.** Some distortion of the cube is noted with the longest distances being associated with the $Rh(CO)_2$ group. In addition, the three phosphinidene groups bound to this metal fragment cap asymmetrically the faces of the cube, with three very long Rh–P distances (average of 2.761(7) Å). The other Rh–P distances range from 2.246(6) to 2.361(7) Å.

In order to gain insight into the electronic structure of compounds **1**–**3**, DFT calculations were conducted on the models $Rh_8(CO)_{12}(\mu_4\text{-GeH})_6$ (**1-H**), $Rh_8(CO)_8(PH_3)_4(\mu_4\text{-GeH})_6$ (**2-H**), and $Rh_8(CO)_9(\mu_4\text{-PH})_6$, (**3-H**). Models containing initially a regular hexacapped cubic core were first optimized without any symmetry constraint. Pertinent metrical parameters are compared with corresponding experimental values in Table 1. For model **1-H**, the 12 Rh–Rh bond distances vary from 2.845 to 2.926 Å with an average distance of 2.899 Å, mimicking quite satisfactorily the Rh–Rh distances (average 2.889 Å) measured experimentally for **1**. The calculated Rh–Ge distances ranging from 2.359 to 2.691 Å are also in a good agreement with those observed experimentally which range from 2.330 to 2.719 Å. In **2-H**, the experimental and computed average Rh–Rh distances equal to 2.949 and 2.950 Å, respectively , are somewhat longer than those observed and calculated for **1-H** with an average Rh–Rh distances equal to 2.906 and 2.916 Å, respectively. The replacement of four strong π-acceptor CO ligands by four weak π-acceptor phosphine ligands hardly perturbs the skeletal $Rh_8(\mu_4\text{-Ge})_6$ core. The geometries, optimized with C_1 symmetry are close to C_{2v} symmetry. The main data are reported in Table 1.

The experimental distances measured in **3** are not so well reproduced in model **3-H**. In the latter the 12 optimized Rh–Rh bond distances vary from 2.866 to 2.922 Å with an average value of 2.899 Å, notably longer than the experimental average value, which is 2.772 Å. Nevertheless, theoretical results show that Rh–P distances involving the $Rh(CO)_2$ group are longer (2.53–2.68 Å) than the other distances, which vary from 2.27 to 2.33 Å. This is in agreement with the corresponding experimental distances (2.53–2.76 Å vs. 2.25–2.36 Å).

The DFT molecular orbital diagram of model **1-H** with idealized C_{2v} symmetry (the actual optimized geometry of C_1 symmetry is very close to C_{2v} symmetry) is shown in Fig. 1 (that of **2-H** is analogous and is not shown here). A large HOMO ($45a_1$) /LUMO ($35b_1$) gap of 1.33 eV is calculated for **1-H** with a count of 114 MVEs, in agreement with the stability of **1** and **2**.

Interestingly, a substantial energy gap of 0.62 eV is computed between vacant molecular orbitals (MO) $46a_1$ and $29a_2$. Occupation of MOs up to $46a_1$ would give a species with 120 MVEs, which is the most favored closed-shell electron count for a regular cubic architecture (see above). Geometry optimization was then performed on the 120-MVE model $\mathbf{[1\text{-}H]^{6-}}$. A comparison of its metrical data with those computed for **1-H** (Table 1) indicates that such an augmentation of the electron count from 114 to 120 leads to substantial lengthening of the Rh–Rh distances. They

Table 1 Optimized geometries of $[Rh_8(CO)_{12}(\mu_4\text{-}GeH)_6]^{n-}$, ($[\mathbf{1\text{-}H}]^{n-}$, n = 0, 6), $Rh_8(CO)_8(PH_3)_4(\mu_4\text{-}GeH)_6$ (**2-H**), and $[Rh_8(CO)_9(\mu_4\text{-}PH)_6]$ (**3-H**) clusters with C_1 symmetry

Compounds MVE count	**1-H** 114	**2-H** 114	**3-H** 114	$[\mathbf{1\text{-}H}]^{6-}$ 120
Bond distances (Å)				
Rh1–Rh2	(2.923) 2.912	(2.942) 2.912	(2.776) 2.812	3.179
Rh2–Rh3	(2.927) 2.926	(2.866) 2.926	(2.763) 2.806	3.171
Rh3–Rh4	(2.865) 2.875	(2.952) 2.875	(2.881) 2.910	3.162
Rh4–Rh1	(2.820) 2.862	(2.862) 2.862	(2.787) 2.846	3.159
Rh5–Rh6	(2.823) 2.842	(2.923) 2.912	(2.717) 2.712	3.179
Rh6–Rh7	(2.939) 2.928	(2.927) 2.926	(2.776) 2.781	3.171
Rh7–Rh8	(2.892) 2.879	(2.865) 2.875	(2.774) 2.779	3.162
Rh8–Rh5	(2.933) 2.938	(2.820) 2.862	(2.712) 2.716	3.159
Rh1–Rh6	(2.923) 2.912	(2.952) 2.912	(2.715) 2.751	3.193
Rh2–Rh7	(2.830) 2.851	(2.939) 2.851	(2.776) 2.811	3.189
Rh4–Rh5	(2.886) 2.893	(2.949) 2.893	(2.886) 2.922	3.187
Rh3–Rh8	(2.825) 2.845	(2.956) 2.845	(2.809) 2.841	3.184
$Rh\cdots Rh_{average}$	(3.205) 3.256	(3.316) 3.321		4.459
Rh-(μ_6-E)	(2.330–2.720)	(2.344–2.826)	(2.246–2.761)	
	2.359–2.691	2.341–2.779	2.274–2.680	2.538
Dihedral angles (°)				
Rh1–Rh2–Rh3–Rh4	25.62	8.45		6.71
Rh5–Rh6–Rh7–Rh8	24.16	9.78		5.88
Angles (°)				
Rh1–Rh2–Rh3	(107.2) 105.2	(101.5) 100.3		89.2
Rh2–Rh3–Rh4	(66.6) 69.4	(78.2) 79.8		90.8

Available experimental distances and angles are given in parenthesis

range now from 3.159 to 3.193 Å (Δd = 0.034 Å) for $[\mathbf{1\text{-}H}]^{6-}$. They were varying from 2.866 to 2.922 Å (Δd = 0.056 Å) in **1-H**. On the other hand the Rh–Ge separations hardly change upon electron addition: 2.359–2.691 Å in **1-H** and 2.447–2.666 Å in $[\mathbf{1\text{-}H}]^{6-}$. The metal–metal lengthening is in agreement with the M–M antibonding character of the three MOs, $35b_1$, $35b_2$, and $46a_1$, which are populated upon the increase of the electron count (see Fig. 2). Importantly, a smaller distortion with respect to the regular cube is computed upon electron addition. As shown in Table 1 and Fig. 3, there is a tendency towards some flatness of the metallic "squares" with dihedral angles decreasing from 25° in the neutral model **1-H** to 7° in the anionic model $[\mathbf{1\text{-}H}]^{6-}$. A lengthening of the Rh–Rh contacts along the "short" diagonals is also computed: from 3.256 Å (av.) in **1-H** to 4.459 Å in $[\mathbf{1\text{-}H}]^{6-}$. Moreover, a look at the angles around the metal atoms indicates also that the faces become more and more regular with angles close to 90°. Although smaller than for the neutral model **1-H**, a substantial HOMO/LUMO gap of 0.74 eV is computed for the optimized geometries of the $[\mathbf{1\text{-}H}]^{6-}$ anion (see Fig. 1).

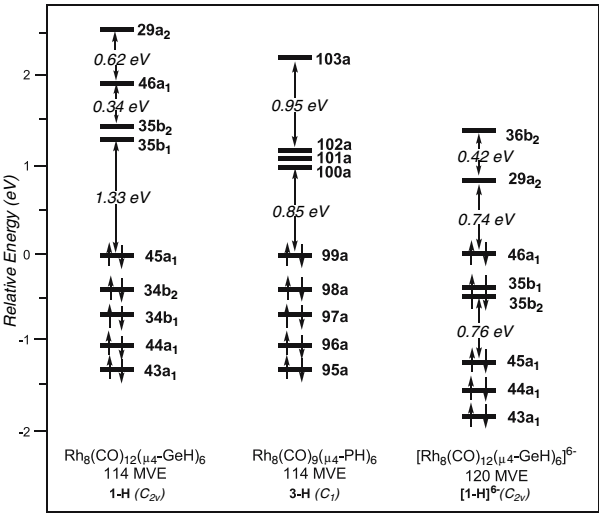

Fig. 1 MO diagrams of **1-H**, **3-H**, and **[1-H]**$^{6-}$. The energy of the HOMOs has been arbitrarily set at 0

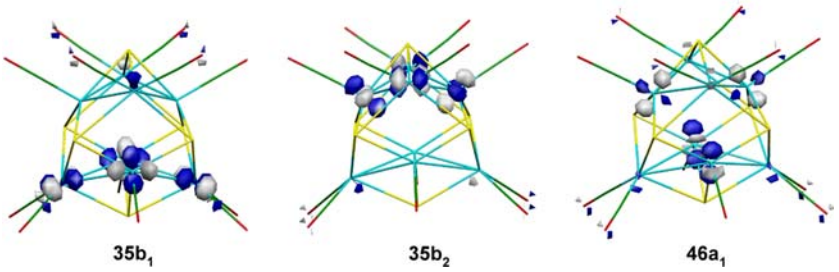

Fig. 2 LUMOs $35b_1$, $35b_2$, and $46a_1$ of **1-H**. Contour values are ±0.06 (e/bohr^3)

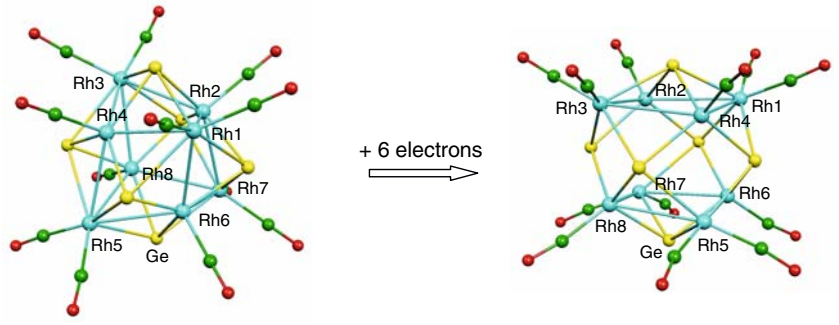

Fig. 3 Optimized molecular structures of **1-H** and **[1-H]**$^{6-}$

Calculations were also carried out on an isomeric form of **1-H**, with four adjacent $Rh(CO)_2$ group and four adjacent Rh(CO) groups. This structure of C_{4v} symmetry, i.e., less distorted than **1-H,** is largely less stable than **1-H** by 25 kcal/mol. This supports the assumption previously mentioned that the distortion of the metallic core in the 114-MVE Rh_8 architectures is mainly caused by the asymmetric ligand environment of the different rhodium atoms.

We now investigate the role played by the existence of different $Rh(CO)_2$ and Rh(CO) fragments in the closed-shell 114-MVE count of **1**, **2**, and **3**, keeping in mind that the best closed-shell electron count of $M_8L_8(\mu_4\text{-E})_6$ or $M_8L_8(\mu_4\text{-ER})_6$ species is 120 MVEs. The removal of a two-electron ligand from the cluster has to be replaced by the addition of two electrons in a nonbonding MO of 4d parentage, thus keeping the 114-MVE count unchanged. This formal operation can be repeated until there are only Rh(CO) fragments on the cluster cage. Actually, this is experimentally illustrated with compounds **1**–**3** which possess the same electron count, 114, but a different number of terminal ligands, either twelve or nine. Indeed, the MO diagram of **3-H**, shown in the middle of Fig. 1 shows a substantial HOMO-LUMO gap for this electron count.

This simple rule was checked by DFT calculations performed on optimized models $Rh_8(CO)_{12-x}(\mu_4\text{-GeH})_6$ (x = 0–4). This is schematized in Fig. 4. Upon each removal of a CO ligand, one Rh–CO antibonding σ^* MO combination is replaced by a metal dsp_σ hybrid MO sufficiently low in energy to be occupied. Although some other vacant levels are also stabilized, a substantial HOMO-LUMO gap (larger than 0.7 eV according to our DFT calculations) is maintained for the count of 114 MVEs. Interestingly, in the case of $Rh_8(CO)_8(\mu_4\text{-GeH})_6$, the fourth vacant σ-type MO, slightly metal–metal antibonding is less stabilized in energy than the other three (see Fig. 1). This leads to a situation where rather large HOMO-LUMO gaps are found for 114 but for 120 MVEs. With electronegative metals such as nickel, ΔE might decrease, favoring the count of 120 MVEs, the expected electron count for regular cubic $M_8L_8(\mu_4\text{-ER})_6$ clusters. Note that the distortion of the cube diminishes with the removal of carbonyl ligands to reach regular O_h symmetry with eight terminal CO groups. In the case of 120-MVE $Ni_8L_8(\mu_4\text{-ER})_6$ species, the t_{2g}

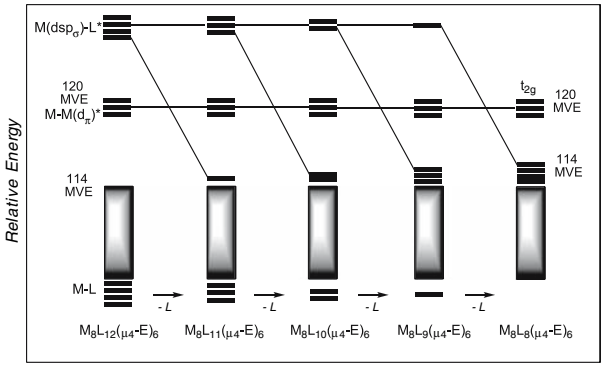

Fig. 4 Qualitative MO diagrams of $Rh_8(CO)_{12\text{-}x}(\mu_4\text{-E})_6$ (x = 0–4) clusters

HOMO lies about 1 eV above the next occupied MOs, because of its (moderate) M–M antibonding character [4, 18]. Thus, although the 114-MVE count is electron-deficient with respect to the EAN (18-electron) and the PSEP theory rules, it is also a closed-shell count for $M_8L_8(\mu_4\text{-ER})_6$ clusters. Such an electron count should be favored with metals less electron-rich (and less electronegative) than Ni. We predict that species of the type $[Rh_8L_8(\mu_4\text{-PR})_6]^{2-}$ or $Rh_8L_4X_4(\mu_4\text{-SR})_6$ (L = CO, PR_3; X = halogen) should be stable enough for being isolated.

One may now wonder what would happen if the formal operation of CO removing was carried on $M_8L_8(\mu_4\text{-ER})_6$. We showed some years ago that when the number of two-electron L ligands is lower or equal than eight, the metal nonbonding MO which is generated is now a high-lying sp hybrid which should remain unoccupied for the closed-shell requirement to be satisfied [4]. Thus, the best closed-shell for $Ni_8L_{8-x}(\mu_4\text{-E})_6$ species is $120-2x$. Starting from the electron-deficient closed-shell count of 114 MVE's for some $M_8L_8(\mu_4\text{-ER})_6$ species, the related closed-shell counts for M_8L_{8-x} $(\mu_4\text{-ER})_6$ would be $114 - 2x$ [4, 18].

Conclusion

The theoretical analysis of the bonding in omnicapped cubic rhodium clusters with more than eight terminal ligands shows an optimal count of 114 MVEs. For such a count, a closed-shell configuration is computed with a substantial HOMO-LUMO gap. The presence of ML_2 instead of ML fragments favors highly distorted cubic architectures with capping ligands asymmetrically bound to the metal square faces. Removal of terminal ligands leads to the replacement of bonding M–L electron pairs by nonbonding electron pairs localized on the metal atoms, giving an unchanged MVE count.

Acknowledgments Thanks are expressed to Prof. R. D. Adams (University of South Carolina) for helpful comments. These studies were facilitated by travel grants from a French-Algerian CNRS-DEF program (2005-17922). Computing facilities were provided by the Pôle de Calcul Intentif de l'Ouest (PCIO) center of the University of Rennes 1 and the Institut de Développement et de Ressources en Informatique Scientifique (IDRIS-CNRS) center of Orsay.

References

1. See for example: (a) J.-F. Halet and J.-Y. Saillard (1997). *Struct. Bond.* **87**, 81. (b) R. Gautier, J.-F. Halet, and J.-Y. Saillard, *in* P. Braunstein, L. Oro, and P. R. Raithby (eds.), *Metal Clusters in Chemistry* (Wiley-VCH, New York, 1999), Vol 3, p. 1643, and references therein
2. (a) K. Wade, *in* B. F. G. Johnson (ed.), *Transition Metal Clusters* (Wiley, Chichester, U.K., 1980), p 193. (b) D. M. P. Mingos and D. J. Wales, *Introduction to Cluster Chemistry* (Prentice Hall International Editions, Englewood Cliffs, NJ, 1990)
3. (a) J. K. Burdett and G. J. Miller (1987). *J. Am. Chem. Soc.* **109**, 4081. (b) G. G. Hoffman, J. K. Bashkin and M. Karplus (1990). *J. Am. Chem. Soc.* **112**, 8705. (c) N. Rösch, L. Ackermann, and G. Pacchioni (1993). *Inorg. Chem.* **32**, 2963
4. E. Furet, A. Le Beuze, J.-F. Halet, and J.-Y. Saillard (1994). *J. Am. Chem.Soc.* **116**, 274
5. (a) E. Furet, A. Le Beuze, J.-F. Halet, and J.-Y. Saillard (1995). *J. Am. Chem. Soc.* **117**, 4936. (b) R. Gautier, F. Ogliaro, J.-F. Halet, J.-Y. Saillard, and E. J. Baerends (1999). *Eur. J. Inorg. Chem.* 1161

6. B. Zouchoune, F. Ogliaro, J.-F. Halet, J.-Y. Saillard, J. R. Eveland, and K. H. Whitmire (1998). *Inorg. Chem.* **37**, 865
7. R. Gautier, J.-F. Halet, and J.-Y. Saillard (1999). *Eur. J. Inorg. Chem.* 673
8. R. D. Adams and J. L. Smith (2005). *Inorg. Chem.* **44**, 4276
9. A. M. Arif, R. A. Jones, D. E. Heaton, C. M. Nunn and S. T. Schwab (1988). *Inorg. Chem.* **27**, 254
10. (a) V. G. Albano, P. Chini, G. Ciani, S. Martinengo, and M. Sensoni (1978). *J. Chem. Soc., Dalton Trans*. 463. (b) J. Rimmelin, P. Lemoine, M. Gross, R. Mathieu, and D. De Montauzon (1986). *J. Organomet. Chem*. **309**, 355
11. V. G. Albano, M. Sensoni, P. Chini, S. Martinengo, and D. Strumolo (1975). *J. Chem. Soc., Dalton Trans*. 305
12. ADF2004.01, *Scientific Computing and Modelling NV, Theoretical Chemistry* (Vrije Universiteit: Amsterdam, The Netherlands, http://www.scm.com)
13. (a) E. J. Baerends, D. E. Ellis, and P. Ros (1973). *Chem. Phys*. **2**, 41. (b) E. J. Baerends, D. E. Ellis, and P. Ros (1978). *Int. J. Quantum. Chem*. **S12**, 169. (c) P. H. Boerrigter, G. te Velde, and E. J. Baerends (1988). *Int. J. Quantum. Chem*. **33**, 87. (d) G. te Velde and E. J. Baerends (1992). *J. Comput. Phys*. **99**, 84. (e) C. Fonseca Guerra, J. G. Snijders, G. te Velde, and E. J. Baerends (1998). *Theo. Chem. Acc*. **99**, 391. (f) G. te Velde, F. M. Bickelhaupt, S. J. A. van Gisbergen, C. Fonseca Guerra, E. J. Baerends, J. G. Snijders, and T. Ziegler, (2001). *J. Comput. Chem*. **22**, 931
14. S. Vosko, L. Wilk, and M. Nusair (1990). *Can. J. Chem.* **58**, 1200
15. (a) A. D. Becke (1986). *J. Chem. Phys*. **84**, 4524. (b) A. D. Becke (1988). *Phys. Rev*. **A84**, 4524
16. (a) J. P. Perdew (1986). *Phys. Rev*. **B33**, 8882. (b) J. P. Perdew (1986). *Phys. Rev*. **B34**, 7406
17. L. Versluis and T. Ziegler (1988) *J. Chem. Phys.* 88, 332
18. DFT calculations on the 120-MVE cluster $Ni_8(CO)_8(\mu_4\text{-}PH)_6$ at the same level of theory as for the title compounds found a gap below the t_{2g} HOMO of 1.3 eV